ISSN 0717-3644
ISSN online 0718-221X

Maderas. Ciencia y tecnología 10(1): 3-18, 2008

DRYING STRATEGIES CAPABLE OF REDUCING THE STRESS LEVEL OF A STACK OF BOARDS AS DEFINED BY A COMPREHENSIVE DUAL SCALE MODEL

***Romain Rémond*[1]*, Patrick Perré*[1]**

ABSTRACT

During drying, stresses and deformations develop in a wood board due to shrinkage fields which result from moisture content and temperature field variations. In spite of numerous works done in wood drying modelling in the last decades, wood drying optimisation based on modelling and simulation remains far from initial expectations. Two main reasons can explain this assessment: the huge variability of wood and the variations in drying conditions throughout the board stack in a dryer.

To address these two key problems, we used a dual scale numerical tool able to compute simultaneously the stress and deformation of hundreds of boards in the stack during drying. A rigorous one-dimensional mechanical formulation, based on previous works, has been used for calculating stress and deformation during drying. The mechanical model is fitted into a module and then added to a dual scale (board-stack) model. This numerical tool has been used to improve the drying schedules recommended by the Technical Centre for Wood and Furniture in France (CTBA) for spruce. The proposed drying schedules allow the board quality to be improved. Note that the optimisation was limited to medium temperature values, so that the proposed schedule can be applied to conventional kilns.

Keywords: Wood drying, stack of boards, dual scale model, drying schedule, drying stress.

INTRODUCTION

Because of the resistances to mass and heat transfer that take place between the air and wood and also within the wood itself, a non-uniform moisture content field develops within the board before the equilibrium moisture content is attained. This field gives rise to a non uniform shrinkage domain which is a source of mechanical stress and shape deformation that could result in surface and/or internal checking.

During the last decades, numerous works have tried to model this behaviour for a single board: Initial, models addressed the coupling between heat and mass transfer in porous media (Stanish *et al.* 1986, Perré and Degiovanni 1990, Perré and Turner 1999), then the stresses and strains induced by the non-uniform shrinkage field (Martensson and Svensson 1997a, b, Mauget and Perré 1999, Pang 2000, Carlsson and Tinnsten 2002). As first goals, cognitive models were used to check whether the simulations could reflect the observed phenomena on a single board during its drying. Gradually, models became able to predict the drying behaviour of a single board over a wide range of drying conditions. Taking the effect of internal gaseous pressure into consideration enabled the model to be extended to "high temperature configurations", those which induce an internal vaporization.

[1]LERMAB, UMR1093, INRA, ENGREF, 14, rue Girardet, F-54042, Nancy, France.
Corresponding author: remond@nancy-engref.inra.fr
Received: 04.12. 2007
Accepted: 29.02. 2008.

However, in spite of the positive results obtained at the single board scale, wood drying optimisation based on modelling and simulation remains far from our ultimate expectations, namely, drying schedule optimisation based on modelling. Note that the drying process optimisation should consider the drying time, the final quality of the products, energy consumption and the global drying cost. Two main reasons can explain this assessment:

- wood is of biological origin, which produces a huge material variability;
- all boards of a stack are in close interaction as a result of their effect on the drying conditions within the stack (Salin 2005, Awadalla *et al*. 2004, Perré and Rémond 2006) and an intricate coupling exists between the stack scale and the board scale.

The first part of this paper presents a numerical tool able to address these two key problems, and to simultaneously compute the stress and deformation of hundreds of boards during drying. The second part provides some simulation results to illustrate how this multi-scale model can be used to improve the drying schedules currently used in the timber industry.

THE NUMERICAL TOOL

Accounting for board-scale coupling

The coupling between scales (board-stack) can be achieved by embedding the information gained from the fine-scale simulation into the coarser scale simulation. A hierarchical approach is adopted where simulations at both scales are performed separately. The local fluxes exchanged between the board and the airflow are calculated using our computational model known as *TransPore*, which solves the coupled heat and mass transfer equations within the board (Fig. 1).

In a batch lumber kiln, boards are arranged in layers, and each board is placed edge to edge on the same tier. Consequently, moisture migration and heat transfer take place mainly in the direction of the board thickness, which results primarily in one-dimensional moisture content and temperature profiles. This allows us to use the very fast 1-D version of *TransPore*, which allows the drying simulation of a 100-board stack to be completed in less than 30 seconds on a 2.8 GHz Xeon processor. The equations and the solving method of the dual scale computational model of a batch lumber kiln are presented in details in Perré and Rémond (2006). A nice agreement experiment results and prediction can be found in Perré *et al.* (2007).

Maderas. Ciencia y tecnología 10(1): 3-18, 2008

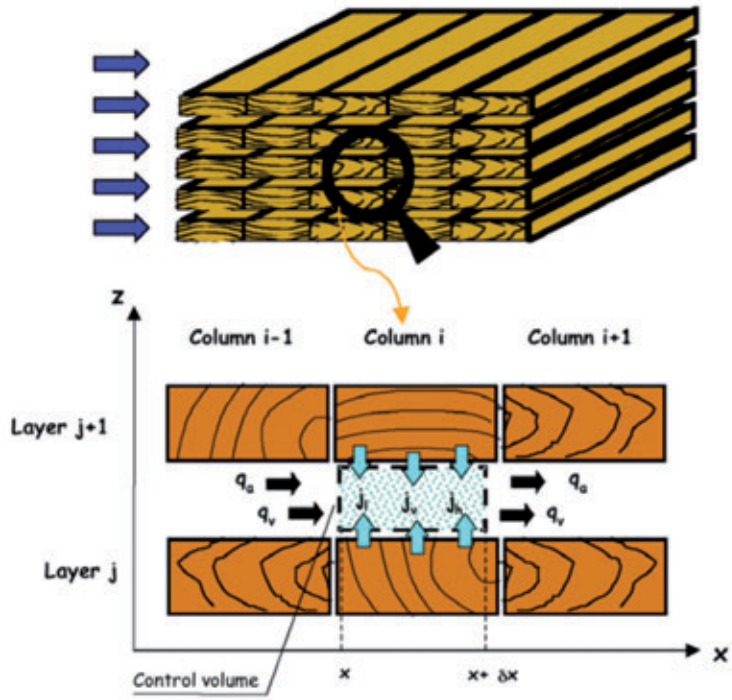

Figure 1. Control volume in the airflow and fluxes at the control faces.

Accounting for wood variability

Since boards come from several trees growing under different environmental conditions, they consist of different composition. In addition, wood properties within the log also present a wide variability (sapwood *vs* heartwood, flatsawn *vs* quatersawn, presence of reaction wood…). Therefore, one can imagine that wood boards within the stack have dramatic variations in their properties, hence in their drying behaviour. In order to account for this variability, a Monte-Carlo method has been implemented to generate the stack which is computed in the dual scale model. The log diameter and the oven-dry density are generated as random variables.

A sample sawing pattern plane, which is used in the wood industry, has been applied to all logs according to their randomly generated diameters. This method is presented in detail in Perré and Rémond (2006) and Perré *et al*. (2006).

Accounting for drying quality

During drying, stresses and deformations develop in the board due to shrinkage. The complex mechanical behaviour of wood includes elasticity, plasticity, viscoelasticity and mechanosorption. In order to take into account the drying quality in the dual scale model, a rigorous one-dimensional mechanical formulation (Rémond *et al.* 2007) was derived from previous 2-D works (Perré and Passard 1995, 2004, Mauget and Perré 1999).

The mechanical problem is formulated in terms of displacement, from which the total strain tensor is derived. The latter is divided in several terms:

$$\overline{\overline{e}}^{tot} = \overline{\overline{e}}^{sh} + \overline{\overline{e}}^{e} + \overline{\overline{e}}^{ms} + \overline{\overline{e}}^{ve} \quad (1)$$

The shrinkage tensor $\overline{\overline{\varepsilon}}^{sh}$ is supposed to be proportional to variations of bound water content, the elastic strain is related to the actual stress tensor via Hooke's law, the viscoelastic strain tensor $\overline{\overline{e}}^{ve}$ uses four thermally activated Kelvin elements and the mechano-sorptive strain tensor $\overline{\overline{e}}^{ms}$ uses the concept of strain limitation (Salin 1992).

The mechanical problem uses a displacement formulation. The total strain tensor is then simply deduced from the displacement field. Introducing equation (1) in the mechanical balance equations produces a set of equations that depend on the displacement field, as well as the temperature and moisture fields. This formulation is implemented into a numerical procedure and added to each module of *TransPore*. At each time increment, temperature and moisture content fields are calculated from the coupled heat and mass transfer equations. The shrinkage field is deduced from these variables and the set of mechanical equations is solved to estimate the displacement field.

IMPROVING DRYING SCHEDULES

In this section, the model presented above was utilized to simulate the drying of the same stack produced by one particular random draw of our stochastic approach. Input values used in the code *TransPore* for heartwood and sapwood boards are presented in Table 1. The stack is composed of 120 boards, 27 mm thick. Each layer of the stack is divided into 12 boards of equal width (200 mm).

Table 1 . Input values used in the code *TransPore* (with S_{fw} the saturation variable in free water).

	Sapwood	Heartwood
Initial MC (%)	180	60
Intrinsic liquid permeability (m^2)	3×10^{-16}	3×10^{-17}
Intrinsic gaseous permeability (m^2)	6×10^{-17}	3×10^{-17}
Relative permeability	$k_{rl} = \left(S_{fw}\right)^{2.28}$ $k_{rg} = 1 + \left(2S_{fw} - 3\right)\left(S_{fw}\right)^2$	
Bound water diffusion	$D_b^T = \left[-9.9 - 9.8X - \frac{4300}{T_K}\right]$ and $D_b^R = 1.2\, D_b^T$	
Gaseous diffusion	$D_{eff}^T = 4.10^{-3}\, k_{rg}\, D_v$	

Maderas. Ciencia y tecnología 10(1): 3-18, 2008

Reference simulation

Table 2. Drying schedule recommended by CTBA (Technical centre for wood and furniture), in France for Norway spruce boards (Aléon *et al.* 1990).

Wood MC (%)	Dry bulb temperature (°C)	Relative humidity (%)	EMC (%)
Vert	70	85	14.5
< 35	70	83	13.7
< 32	70	72	10.8
< 30	75	65	8.7
< 28	75	60	7.8
< 25	75	50	6.5
< 20	80	40	5
< 15	80	28	3.8

The drying schedule used for these tests is applied in many factories throughout France for Norway spruce (Table 2) in which the air conditions evolve according to the average moisture content of the stack. The air velocity is set equal to 2.5 $m.s^{-1}$ and the stick thickness is 20 mm. Simulation 1 is performed with a constant airflow direction during all the drying process, Figure 2-a presents the evolution of the drying conditions at the stack inlet, as obtained as a result of the drying schedule and the drying kinetics of each board of the stack. It is interesting to notice that the kinetics of sapwood and heartwood boards are getting closer as drying progresses (Fig. 2-b): this is the well-known opposite effect of lower initial moisture content and lower permeability in heartwood. This difference in behaviour becomes evident when plotting the drying curves that is, drying rate *versus* moisture content. A constant drying rate period clearly appears for sapwood boards, whereas the drying rate of heartwood boards starts to decrease just after the heating-up period (Fig. 3). Notice also that similar boards, of either heartwood or sapwood, may present different drying rate, namely at the beginning of drying. This explains why several drying kinetics cross each other. This is the expression of the stack effect, which explains the difference of the drying rate between the stack inlet and the stack outlet for a same kind of board (sapwood or heartwood). Whatever the board type and the stack position, a peak in the drying rate appears at each climatic change in the drying schedule. As a result of the stack effect, these peaks appear at higher moisture content (MC) for boards located at the stack outlet.

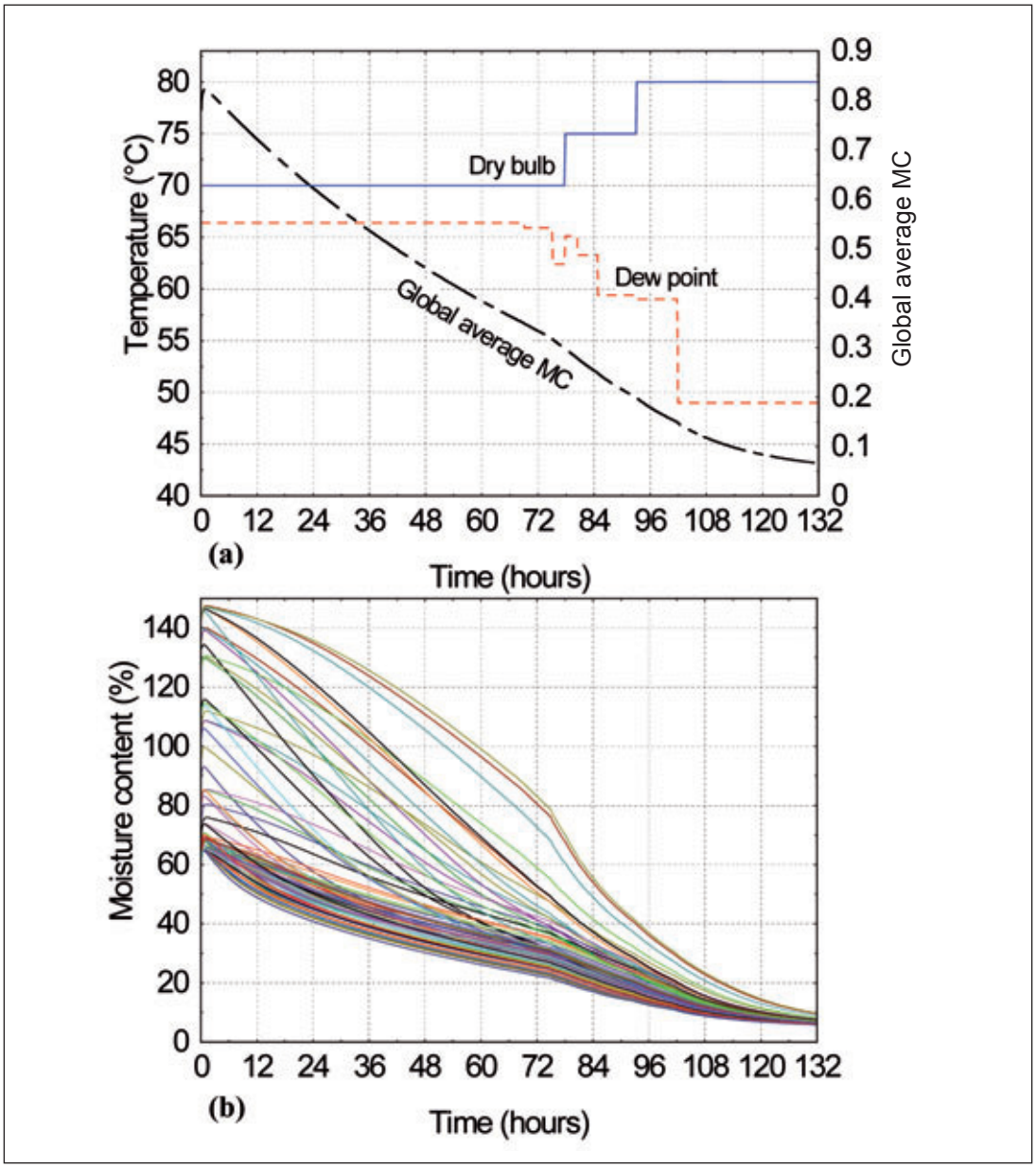

Figure 2. Evolution of air conditions at the stack inlet (a), and drying kinetics of the 120 boards (b) (SIMULATION 1).

Maderas. Ciencia y tecnología 10(1): 3-18, 2008

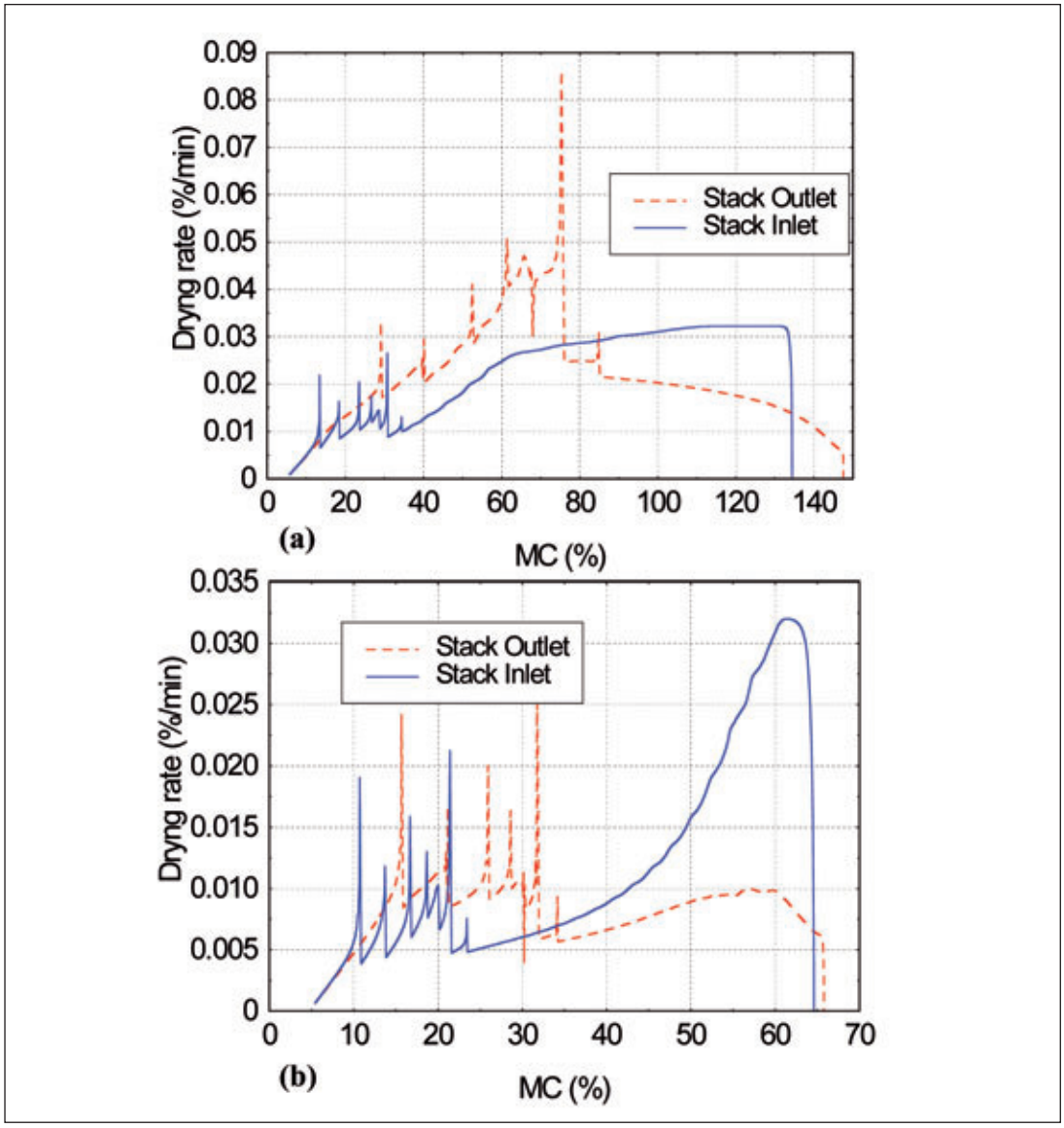

Figure 3. Drying rate of two sapwood boards (a) and two heartwood boards (b) for the drying schedules without airflow reversal (SIMULATION 1).

Impact of airflow reversal

In industrial drying, it is well known that reversing the airflow direction allows a more homogenous MC distribution within the stack to be obtained. To this end, many kiln manufacturers advise that the airflow direction be reversed every hour or two hours. As a result of the air parameters evolving with the airflow, this leads to the periodical application of new drying conditions to the board. The variations of the drying conditions along the airflow direction depend on the stickers thickness, the air velocity, the fluxes of heat and mass exchanged between the air and the boards. Regarding the drying time and drying quality, it is not obvious how to explain the effect of airflow reversal during the drying process. This section aims at answering this troublesome question.

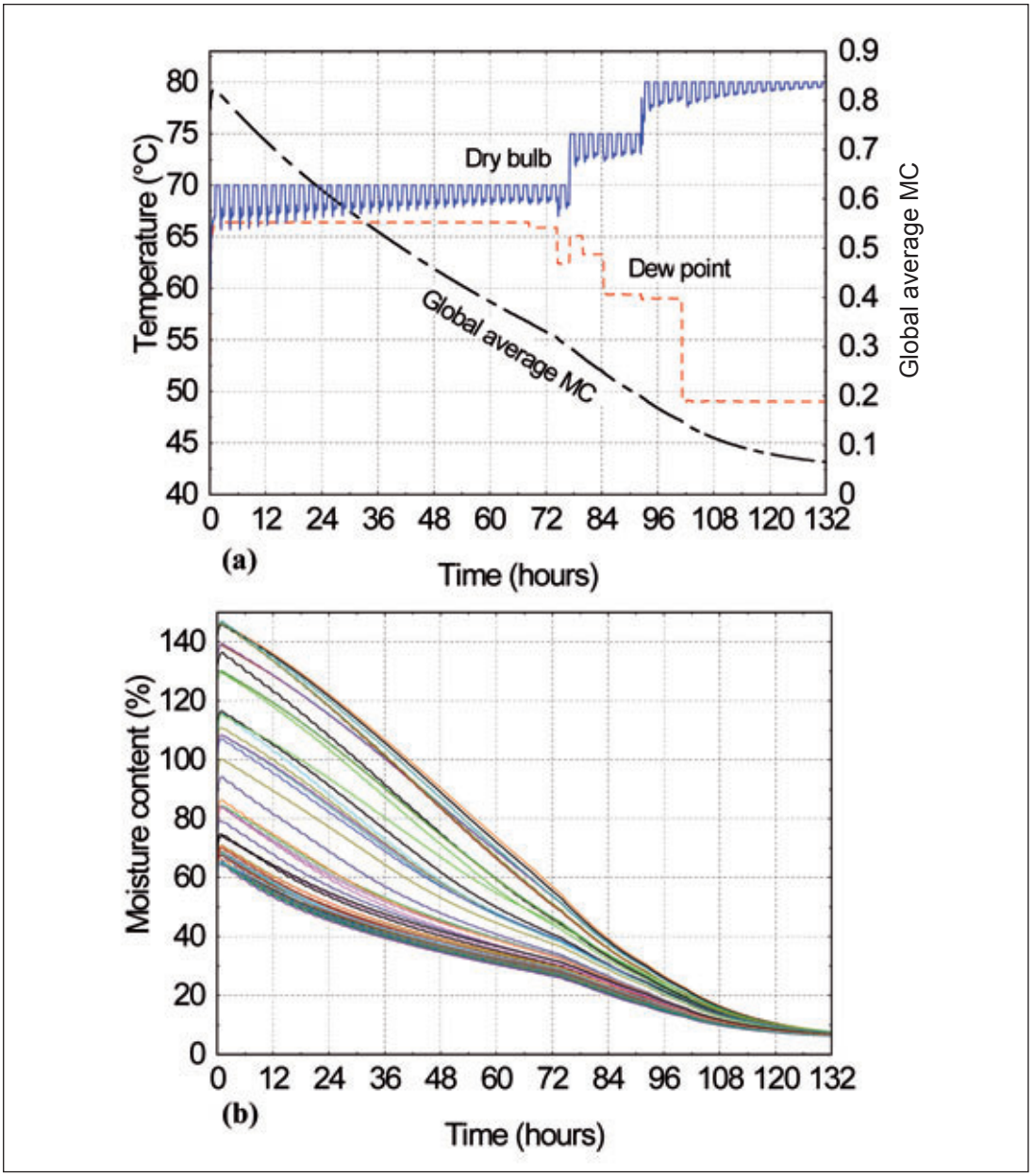

Figure 4. Evolution of air conditions at the stack inlet (a), and drying kinetics of the 120 boards (b) (SIMULATION 2).

Simulation 2 uses the same drying schedule and the same stack of boards as in simulation 1, except that the airflow is reversed each hour. In this case, due to air flow reversal, the drying conditions at one stack edge change periodically with the airflow direction, which explains the oscillations of the dry bulb temperature (Fig. 4-a). The intensity of the oscillations decreases progressively during drying because the fluxes of heat and mass exchanged between the airflow and the boards also decrease as drying progresses. The stack effect therefore reduces as drying progresses. Comparing to simulation 1, the drying kinetics of all boards are now perfectly staggered (Fig. 4-b), namely, the airflow reversal conceals almost all the stack effect .

Maderas. Ciencia y tecnología 10(1): 3-18, 2008

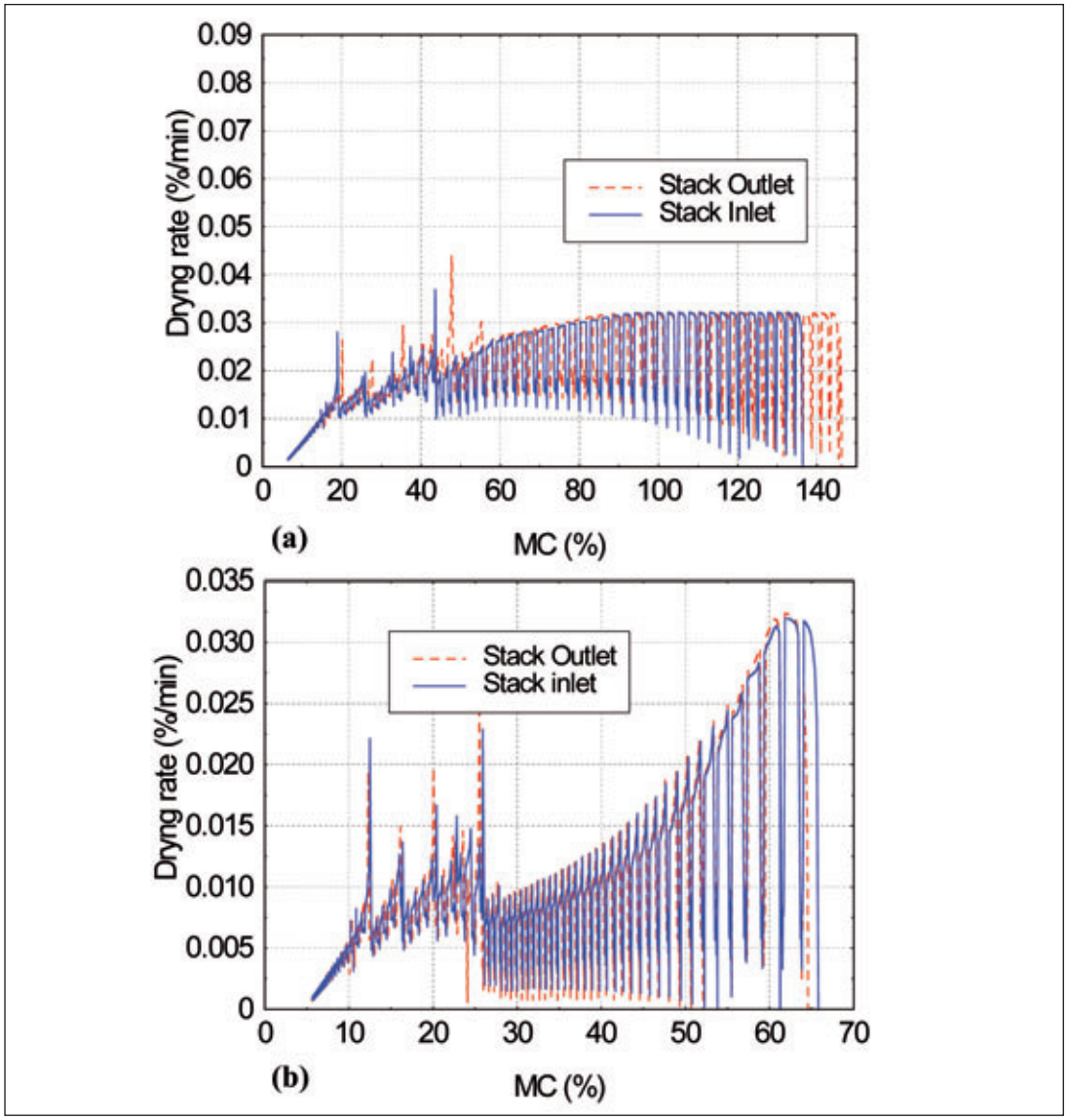

Figure 5. Drying rate of two sapwood boards (a) and two heartwood boards (b) (SIMULATION 2).

Figure 5 shows that the effect of the board location on the drying rate curve disappears when the air flow is periodically reversed. Indeed, the drying rate of each board oscillates, at each airflow reversal, between the inlet and outlet curve of simulation 1 presented in figure 3. Accordingly, all boards have a similar value of the averaged drying rate and the dispersion of MC curves is reduced considerably compared to the test performed without airflow reversal. The total drying time with airflow reversal, for the same final average MC, is shorter than (or at least equal to) the same test performed with constant airflow direction. Various reversing periods were tested, from 0.5 h to 72 h, and this phenomenon was always observed (Table 3). But the lowest deviation around the final target MC is obtained with the shortest period.

Table 3. Simulated results for different reversal periods of airflow, in comparison with results computed without airflow reversal (: total drying time for a target MC of 12%, 107.4 h; standard deviation of final MC, 2.95% ; average value of maximum stress at the surface 1.57 MPa ; average of the absolute value of the surface stress, 0.61 MPa).

Reversal Period	0.5h	1h	3h	6h	12h	24h	48h	72h	Without
Relative total drying time	98.4%	99.3%	99.6%	99.5%	99.4%	99.3%	99.4%	99.9%	100%
Relative Standard deviation of MC	70.4%	71.0%	70.7%	69.8%	70.1%	71.5%	76.3%	84.7%	100%
Relative Maximum surface stress	87%	89%	94%	97%	99%	100%	101%	98%	100%
Relative Absolute value of surface stress	63%	67%	77%	84%	89%	93%	96%	98%	100%
Max final MC (%)	17.23	17.41	17.39	17.27	17.19	17.84	19.39	21.87	23.96
Min final MC (%)	10.23	10.15	10.13	10.13	9.91	9.78	9.63	9.59	8.86

Mechanical quality

Boards located at the stack inlet present more checks than average because they dry in more severe conditions. It is therefore easy to understand why airflow reversal, which leads to middle drying conditions for half the drying time, reduces the stress level of these boards (Fig. 6).

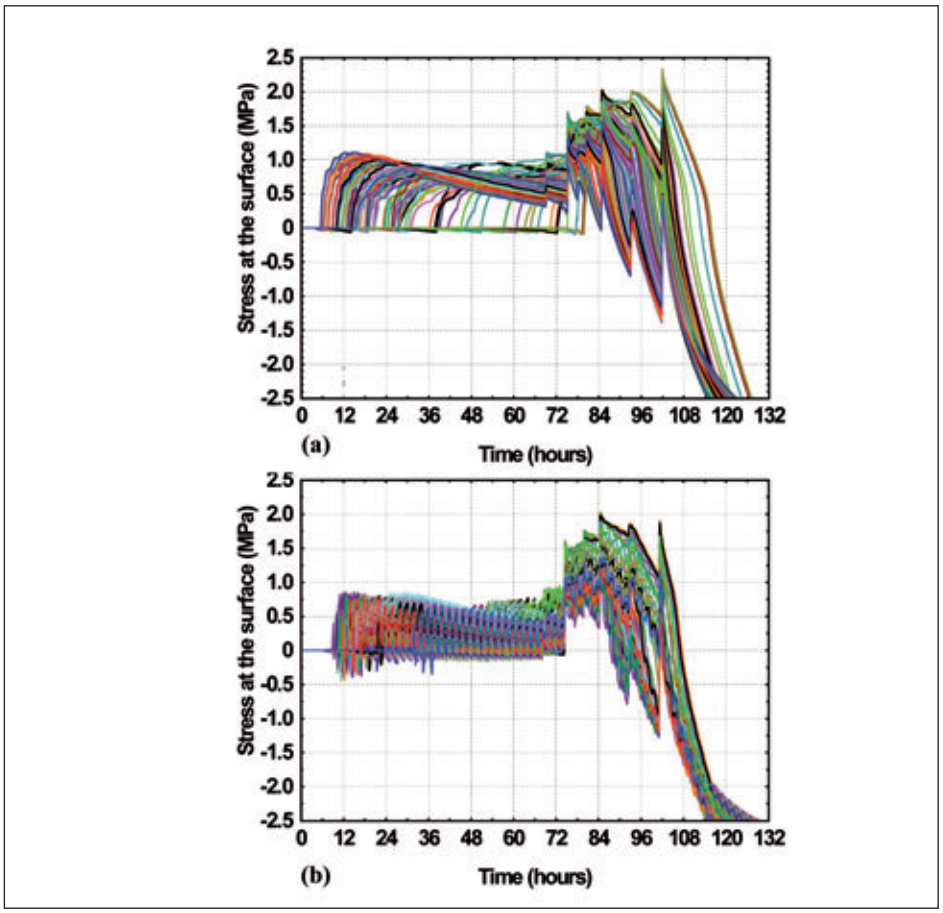

Figure 6. Stress at 1mm beneath the surface of the boards with a constant airflow direction (SIMULATION 1) (a), with an airflow whose direction is reversed each hour (SIMULATION 2) (b).

Maderas. Ciencia y tecnología 10(1): 3-18, 2008

However, a more subtle effect contributes even more to the reduction of the stress level. At the beginning of drying, the periphery of the board is under traction and its MC tends rapidly toward the equilibrium moisture content (EMC) for a constant airflow direction. The mechanosorptive deformation, which results from the coupling between stress and sorption/desorption phenomena, does not evolve any more once the EMC is attained. In the case of airflow reversal, the oscillations of the air conditions lead to alternate sorption/desorption phases near the surfaces of the boards. Because the MC changes continuously near the surface, mechanosorptive creep continues to be activated. This deformation contributes to the reduction of the stress level at the periphery of the board section. This stress reduction affects mainly the first boards located at the stack inlet or outlet. Considering the average of absolute surface stress value, this reduction was observed for all the reversal periods from 0.5h to 72h (Table 3). However, for reversing periods longer than 12h, the activation of mechanosorptive creep is no longer effective and each reversing induce a step change in the drying conditions of boards located at the stack inlet or outlet which increases the stress beneath the surface.

Activation of the viscoelastic properties

By activating viscoelastic creep, it is possible to reduce the stress level, hence surface checks. Indeed, the viscoelastic and mechanosorptive strains contribute to reducing drying stress in the board. In this sense, the activation of viscoelastic creep by increasing the wood temperature as soon as possible is one of the possible ways to reduce the stress level. Obviously, this strategy works only for species which are not prone to collapse. Unfortunately, the glass transition temperature increases dramatically when the bound water content decreases. This fact requires the schedule to account for both temperature and moisture content levels.

The possibility to adjust thermo- and hydro-activation was our guideline to change the drying schedule presented in Table 2. Obviously, schedule changes must consider the technical limits of conventional kilns (heating power, thermal losses, condensation on internal walls, etc.). The schedule proposed in Table 4 uses a higher temperature and equilibrium moisture content than Table 2 at the beginning of drying. The air flow direction is reversed each hour. In addition, the changes in climatic conditions (Table 4) are no longer stepwise but proportional to the difference between the actual global average MC ($\overline{MC}$) and the transition MC of line *i* (MC_i) in the proposed drying schedule. For example when the actual average MC ($\overline{MC}$) is in the range $[MC_i ; MC_{i+1}]$ the set values of temperature or relative humidity are given by:

$$T = a \cdot T_i + (1-a) \cdot T_{i+1} \quad (2)$$

$$RH = a \cdot RH_i + (1-a) \cdot RH_{i+1} \quad (3)$$

with $a = \left(MC_{i+1} - \overline{MC}\right) / \left(MC_{i+1} - MC_i\right)$

Table 4. Drying schedule suggested by this work for spruce.

Wood MC (%)	Dry bulb temperature (°C)	Relative humidity (%)	EMC (%)
Vert	75	85	14.0
< 35	75	83	13.3
< 32	75	78	11.4
< 30	78	71.4	9.7
< 28	80	69	9
< 25	80	63	8
< 20	80	53	6.5

This schedule results in a considerable reduction, by about 43%, of the global average stress beneath the exchange surface in comparison with Table 2 (Fig. 7-a). The total drying time, to reach an average MC of 12 %, is 108 hours for Table 4 against 107 hours for Table 2. The standard deviation in final moisture content in the stack is reduced from 2.95% to 1.2%.

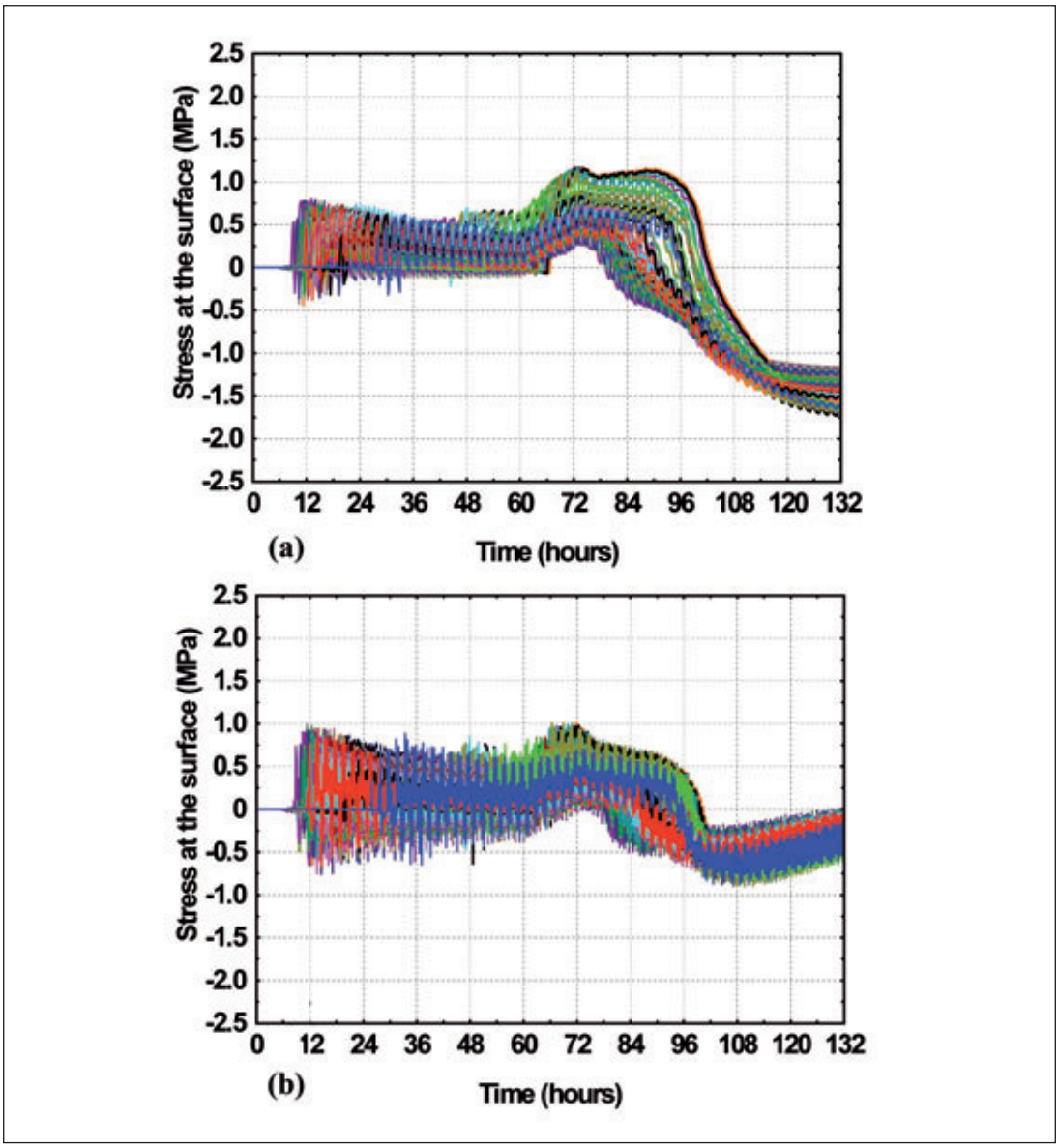

Figure 7. Stress at 1mm beneath the surface of the boards with the proposed drying schedule (table 4) (a), and this schedule with a superimposed oscillation on the dew point temperature (oscillation period : 0,5 h) (b).

Maderas. Ciencia y tecnología 10(1): 3-18, 2008

Activation of the mechanosorptive properties

Some works (Luikov 1968, Langrish et al. 1992, Riehl and Wehling 2003, Salin 2003, Sackey et al. 2004) showed that oscillating climate, based on oscillation of temperature or relative humidity, could improve the final drying quality of the product by enhancing mechanosorptive creep.

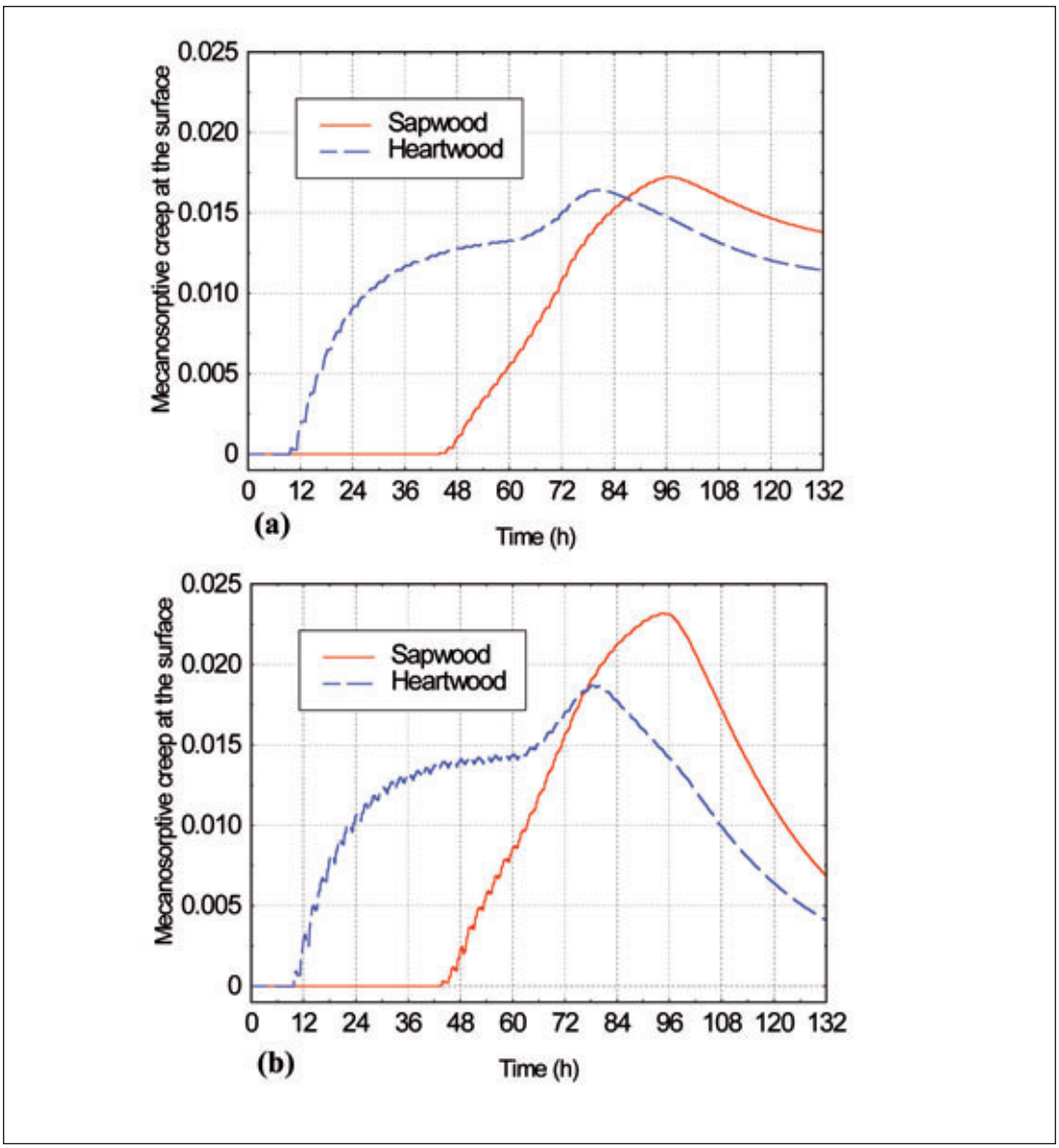

Figure 8. Mechanosorptive creep at 1mm beneath the surface of a sapwood and a heartwood boards when the drying schedule table 4 is applied (a), and this schedule with a superimposed oscillation on the dew point temperature (oscillation period : 0,5 h) (b). Both schedules have an airflow reversed each hour.

In this part, we used this idea to further reduce drying stress in the boards. The previous drying schedule (Table 4) is used with a superimposed oscillation on the dew point temperature of +/-1°C around the desired value. Because the oscillation frequency is short compared to the time constant related to diffusion, the climate oscillations affect only the MC near the board surface. These MC changes produce an additional mechanosorptive creep of the surface layer (Fig. 8). Different oscillation periods have been simulated for 30 min, 60 min and 90 min. The schedule with an oscillation period of 30 min results in a considerable reduction, by about 30%, of the average absolute stress value beneath the exchange surface in comparison with Table 4 (Fig. 7-b). For longer periods, 60 min and 90 min, the activation of mechanosorptive creep is less effective and the average absolute surface stress value is reduced to 25% and 20% respectively, in comparison with Table 4. The total drying time using this oscillating climate is equal to the one obtained in table 4. Indeed, this oscillation frequency only affects a thin peripheral layer on the surface of the board. Actually, more comprehensive work needs to be done in this field due to some controversial results observed experimentally with oscillating climate (Terziev *et al*. 2002). The theoretical results obtained in this part have to be considered like a trend which should be validated by experiments.

CONCLUSION

A dual scale computational model was used to improve the drying schedule recommended for Norway spruce by CTBA (the French technical centre for wood and furniture). Each single board of the stack was simulated using one module of *TransPore*. The meta-model deals with the coupling between these hundreds of boards and the airflow between board tiers. The input data of this model is generated by a stochastic method in order to account for timber variability.

At first, the model was applied to the same stack to elucidate the effect of airflow reversal on the drying time and the drying quality. The computational model confirmed that reversing the airflow dramatically decreases the distribution of MC in the stack, and reduces the risk of checks for boards located at the stack inlet.

Then, based on viscoelastic and mechanosorptive creep activation, a new drying schedule was developed with the aid of the model to obtain fast drying with high quality. A significant reduction, about 60%, in the global average stress level beneath the exchange surface was achieved compared to the initial schedule. The model allows also the best compromise between the reduction of surface stress level and the final stress reversal to be tuned.

These selected simulation tests emphasise the potential of the model addressing industrial issues. This potential lies in the unique capability of this dual-scale model to deal with timber variability and the stack effect simultaneously.

Maderas. Ciencia y tecnología 10(1): 3-18, 2008

REFERENCES

Aléon, D.; Chanrion, P.; Négrié,G.; Perez, J.; Snieg, O. 1990. *Séchage du bois*. Guide Pratique, CTBA, Paris.

Awadalla, H.S.F; El-Dib, A.F.; Mohamad, M.A.; Reuss, M.; Hussein, H.M.S. 2004. Mathematical modelling and experimental verification of wood drying process. *Energy Conservation and Management* 45: 197-207.

Carlsson, P. ; Tinnsten, M. 2002. Optimisation of drying schedules adapted for a mixture of boards with distibution of sapwood and heartwood. *Drying Technology* 20(2): 403-418.

Luikov, A. 1968. *Theory of drying*. Edited by Energia, Moscow.

Langrish, T.A.G.; Keey, R.B.; Kumar, M. 1992. Improving the quality of timber from read beech (N. fusca) by intermittent drying. *Drying Technology* 10(4): 947-960.

Mauget, B.; Perré, P. 1999. A large displacement formulation for anisotropic constitutive laws. *European Journal of Mechanics - A/Solids* 18: 859-877.

Martensson, A.; Svensson, S. 1997 a. Stress-Strain Relationship of Drying Wood. Part 1: developpment of a constitutive Model. *Holzforschung* 51: 472-478.

Martensson, A.; Svensson, S. 1997 b. Stress-Strain Relationship of Drying Wood. Part 2: Verification of a One-Dimensional Model and development of a two-Dimensional model. *Holzforschung* 51: 565-570.

Pang, S. 2000. Modelling of stress development during drying and relief during steaming in Pinus Radiata lumber. *Drying Technology* 18(8): 1677-1696.

Perré, P.; Degiovanni, A. 1990. Simulation par volumes finis des transferts couplés en milieux poreux anisotropes: séchage du bois à basse et à haute température. *Journal of Heat and Mass Transfer* 33(11) : 2463-2478.

Perré, P.; Passard, J. 1995. A control-volume procedure compared with the finite-element method for calculating stress and strain during wood drying. *Drying Technology* 13(3): 635-660.

Perré, P.; Turner, I. W. 1999. A 3-D version of TransPore: a comprehensive heat and mass transfer computational model for simulating the drying of porous media. International *Journal of Heat and Mass Transfer* 42: 4501-4521.

Perré, P.; Passard, J. 2004. - A physical and mechanical model able to predict the stress field in wood over a wide range of drying conditions. *Drying Technology Journal* 22 (1&2): 27-44.

Perré, P.; Rémond, R. 2006. A dual scale computational model of kiln wood drying including single board and stack level simulation. *Drying Technology Journal* 24: 1069-1074.

Perré, P.; Aléon, D.; Rémond, R. 2007. Energy saving in industrial wood drying addressed by a multi-scale computational model: board, stack and kiln. *Drying Technology Journal* 25: 75-84.

Perré, P.; Turner, I.; Rémond, R. 2006. Comprehensive drying models based on volume-averaging: background, application and perspective. *Modern Drying Technology*, volume 1: modelling. Wiley. New York: 66p.

Rémond, R.; Passard, J.; Perré, P. 2007. The effect of temperature and moisture content on the mechanical behaviour of wood: A comprehensive model applied to drying and bending. *European Journal of Mechanics* 26 (3): 558-572.

Riehl, T.; Welling, J. 2003. Taking advantage from oscillating climate conditions in industrial timber drying processes. *8th International, IUFRO Wood Drying Conference*, Brasov, Romania, 24.-29 August : 171-177.

Sackey, E.K.; Avramidis, S.; Oliveira, L.C. 2004. Exploratory evaluation of oscillation drying for thick hemlock timbers. *Holzforschung* 58: 428-433.

Salin, J.G. 1992. Numerical prediction of checking during timber drying and a new mechanosorptive creep model. *Holz als Roh-und Werkstoff* 50: 195-200.

Salin, J.G. 1999. Simulation Models; From a Scientific Challenge to a Kiln Operator Tool. *6 th International IUFRO Wood Drying Conference*, Stellenbosch, South Africa, January: 25-28.

Salin, J.G. 2003. A theoretical analysis of timber drying in oscillating climates. *Holzforschung* 57(4): 427-432.

Salin, J.G. 2005. The Influence of some Factors on the Timber Drying Process, Analysed by a Global Simulation Model. *Maderas.Ciencia y tecnologia* 7(3): 195-204.

Stanish M.A.; Schajer G.S.; Kayihan F. 1986. A mathematical model of drying for porous hygroscopic media. *AIChE Journal* 32(8): 1301-1311.

Terziev, N.; Salin, J.G.; Söderström, O.; Rosenkilde, A.; Temnerud, E. 2002. Oscillation drying of Scots pine timber. *4th COST E15 Worshop "Methods for Improving Drying Quality of Wood*", Santiago de Compostela , Spain, 30-31 May.